Oscillatory shear flow behaviour of a thermotropic liquid-crystalline polymer

Seung Su Kim and Chang Dae Han*

Department of Chemical Engineering, Polytechnic University, Brooklyn, NY 11201, USA

(Received 23 December 1992; revised 13 April 1993)

The oscillatory shear flow properties, dynamic storage and loss moduli (G' and G''), of a thermotropic liquid-crystalline polymer (TLCP) in both the isotropic and nematic regions were measured as functions of angular frequency (ω), using a cone-and-plate rheometer. For the study, an aromatic polyester, poly[(phenyl sulfonyl)-*p*-phenylene 1,10-decamethylene-bis(4-oxybenzoate)] (PSHQ10), was synthesized in our laboratory. The PSHQ10 was found to have (1) a glass transition temperature of 88°C, (2) a melting point of 115°C, and (3) a nematic-to-isotropic transition temperature of 175°C. We found that the oscillatory shear flow properties of PSHQ10 in the nematic region were strongly dependent on its thermal history (i.e. annealing temperature and the duration of annealing) and shear history. Thus, in order to completely erase the thermal history associated with polymerization and sample preparation, a solvent-cast PSHQ10 specimen was first heated to the isotropic region (e.g. 190°C), sheared there at a very low shear rate (0.0085 s^{-1}) for ~5 min, and then cooled very slowly down to a predetermined temperature (130, 140, 150, 160 or 170°C) in the nematic region. We found that in the isotropic region time–temperature superposition holds and plots of $\log G'$ *versus* $\log G''$ give rise to a temperature-independent correlation. On the other hand, we found that in the nematic region *preshearing* has a profound influence on the oscillatory shear flow properties and $\log G'$ *versus* $\log G''$ plots show temperature dependency. This suggests that time–temperature superposition would not hold in the nematic region of PSHQ10 (and also of other types of TLCPs). We thus conclude that $\log G'$ *versus* $\log G''$ plots are very sensitive to variations in the morphological state of PSHQ10 as the temperature varies in the nematic region. We found that the Cox–Merz rule holds for PSHQ10 in the isotropic region and the morphological state of a specimen plays an important role in determining whether or not the Cox–Merz rule holds in the nematic region; specifically an *unsheared* specimen does not follow the Cox–Merz rule, whereas a *sheared* specimen does.

(Keywords: oscillatory shear flow; storage modulus; loss modulus)

INTRODUCTION

A better understanding of the rheological behaviour of thermotropic liquid-crystalline polymers (TLCPs) is essential for the successful processing of such polymers. In recent years, several research groups[1–15] have reported on the transient and/or steady shear flow behaviour of certain TLCPs. However, relatively few studies[2,15–18] have been reported of the oscillatory shear flow behaviour of TLCPs. In the investigation of the rheological behaviour of TLCPs, measurements of oscillatory shear flow properties have certain advantages over measurements of steady shear flow properties; specifically, (1) the time evolution of the morphological state in the nematic region of a specimen, after being subjected to transient or steady shear flow, can be monitored in terms of the dynamic storage modulus (G') or complex viscosity ($|\eta^*|$), by applying small amplitude oscillatory deformations, and (2) oscillatory shear flow measurements allow us to apply much higher angular frequencies, as compared to steady shear flow measurements which are limited to low shear rates when dealing with very viscous molten polymers.

*To whom correspondence should be addressed at Department of Polymer Engineering, The University of Akron, Sidney L. Olson Research Center, Akron, OH 44325-0301, USA

Very recently we have embarked on an investigation of the rheological behaviour of TLCPs. In this endeavour, we have synthesized a thermotropic polyester, poly[(phenyl sulfonyl)-*p*-phenylene 1,10-decamethylene-bis(4-oxybenzoate)] (PSHQ10), with the chemical structure[19]:

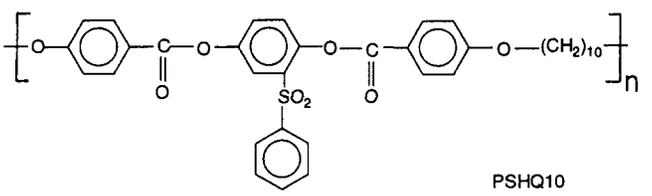

PSHQ10

Previously, Driscoll and co-workers[15,20,21] reported the rheological behaviour of a thermotropic polyester having a chemical structure similar to that of PSHQ10, which had been synthesized by Furukawa and Lenz[19]. It should be mentioned that the number 10 in PSHQ10 refers to the number of methylene units present, i.e. decamethylene or $(CH_2)_{10}$. This convention is chosen in order to distinguish PSHQs with varying numbers of methylene units as flexible spacers. In a future study we intend to synthesize PSHQs with varying lengths of flexible spacers, e.g. PSHQ8 with $(CH_2)_8$ and PSHQ12 with $(CH_2)_{12}$.

0032-3861/94/010093-11

In the investigation of the rheological behaviour of TLCPs, PSHQ10 has some unique features, namely (1) PSHQ10 is a homopolyester, thus allowing us to offer a much simpler interpretation of rheology–morphology relationships, as compared to the situations which deal with copolyesters, such as copolyesters of hydroxybenzoic acid (HBA) and poly(ethylene terephthalate) (PET), and copolyesters of HBA and 2-hydroxy-6-naphthoic acid (HNA); (2) PSHQ10 has a relatively low nematic-to-isotropic transition temperature ($T_{NI}=175°C$, also referred to as the clearing or isotropization temperature), which is significantly lower than the thermal degradation temperature ($\sim 350°C$), thus allowing us to take rheological measurements in both the isotropic and nematic regions; (3) PSHQ10 has a 60°C range between the melting point (115°C) and T_{NI} (175°C), thus enabling us to take rheological measurements over a reasonably wide range of temperatures in the nematic region. Owing to the fact that the T_{NI} of PSHQ10 is much lower than the thermal degradation temperature, in our previous study[22] we have shown how the initial morphology of PSHQ10 in the nematic region can be controlled, which is very important for the investigation of transient shear flow behaviour.

In this paper we shall present the results of our recent study on the oscillatory shear flow behaviour of PSHQ10 in both the isotropic and nematic regions. Emphasis will be placed on pointing out that both thermal and shear histories have a profound influence on the oscillatory shear flow behaviour of PSHQ10 in the nematic region.

EXPERIMENTAL

Polymer synthesis

In the present study PSHQ10 was synthesized via solution polymerization, in our laboratory, by preparing two monomers, 2-phenylsulfonyl-1,4-hydroquinone (A) and 4,4′-dichloroformyl-1,10-diphenoxydecane (B), with the chemical structures[19]:

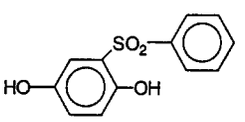

2-phenylsulfonyl-1,4-hydroquinone (A)

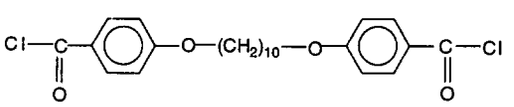

4,4'-dichloroformyl-1,10-diphenoxydecane (B)

Monomer A was prepared by reacting at room temperature a solution of an excess amount of sodium benzenesulfinate in a 5:1 mixture of water and acetic acid with a solution of *p*-benzoquinone (purified by sublimation) in a 5:1 mixture of water and acetic acid. The crude product, precipitated in white powdery form, was filtered and washed with water several times, and then dissolved in methanol and recrystallized from a methanol/water mixture several times. After being dried *in vacuo*, the product was then recrystallized from an ethanol/water mixture several times.

The preparation of monomer B required three steps. (1) 4,4′-Dicarbomethoxy-1,10-diphenoxydecane was prepared by reacting methyl-4-hydroxybenzoate dissolved in *N,N*-dimethylformamide (DMF) with 1,10-dibromodecane in the presence of anhydrous sodium carbonate. The reaction took place with stirring for 4 h in a 2 litre three-necked flask, which was immersed in an oil bath maintained at 135°C. The reaction mixture was cooled and poured into cold water, and then placed in a refrigerator overnight. The crude material was later filtered and washed thoroughly with water and dried. (2) 4,4′-Dicarboxy-1,10-diphenoxydecane was prepared by pouring the reaction product obtained in step 1 into a 10 wt% solution of potassium hydroxide in ethanol. The resulting suspension was stirred with reflux for 4 h and then diluted with water and, finally, heated to 90°C, thus dissolving the potassium salt in the product. Hydrochloric acid solution was added to the solution containing the reaction product until the mixture became distinctly acidic. The solution was allowed to cool overnight before being filtered. The crude product was washed with water and recrystallized several times from a DMF/ethanol mixture. (3) Due to the air-sensitivity of the chlorinated compound, monomer B, chlorination of the product obtained in step 2 (hereafter referred to as Pre-B) was performed immediately before the polymerization to avoid chemical changes of functional groups in both ends of Pre-B during storage. A precise amount of Pre-B was refluxed with thionyl chloride for 4 h, yielding monomer B. Excess thionyl chloride was then removed under reduced pressure for several days.

Monomers A and B in equimolar quantities were stirred in a mixture of dichloromethane and pyridine. Moisture-free and oxygen-free argon gas was kept flowing into the reactor for 2 days. The reactor was then sealed and stirred for 2 days to obtain the maximum degree of polymerization. The polymer was fractionated by precipitating several times in a mixture of methanol and dichloromethane. High molecular weight fractions precipitated in the form of white fibrils and low molecular weight fractions were obtained in the form of a fine powder. A fibrous product was recovered by filtration using a coarse screen followed by washing several times with a methanol/water mixture and drying in a vacuum oven for several days.

Characterization of PSHQ10

The chemical structure of PSHQ10 was confirmed via two-dimensional high-resolution n.m.r. spectroscopy. The samples were prepared in $CDCl_3$ and spectra were acquired at room temperature on a Varian Instruments Gemini 200 n.m.r. spectrometer operating at 200 MHz for ^1H and 50 MHz for ^{13}C. The n.m.r. peak assignments for PSHQ10 are summarized in *Table 1*. The ^1H COSY was acquired as a 256×512 data set and zero filled to 512×512 real points. It was apodized with a sine bell in both dimensions. The COSY was symmetrized after inspection of the data to assure no complications from T_1 noise. Since the major limitation in the ^1H COSY is that there are so many unprotonated carbons in the molecule, we used ^{13}C n.m.r. which would observe all 20 of the different types of carbon. The ^{13}C chemical shifts are characteristic of the structure, but do not provide sufficient information to confirm the structure since a number of the peaks are quite close to each other, e.g. f and s (*Table 1*). Therefore we used a two-dimensional

Table 1 N.m.r. peak assignments for PSQH10

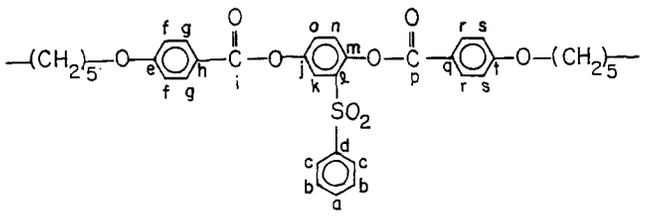

Assignment	^1H	^{13}C
a	7.75	133.90
b	7.30	129.40
c	7.80	128.50
d	–	140.81
e	–	164.40
f	7.05	114.98
g	8.16	132.97
h	–	121.12
i	–	164.87
j	–	148.70
k	7.52	128.90
l	–	134.55
m	–	146.30
n	7.24	126.45
o	8.15	123.75
p	–	163.90
q	–	120.85
r	8.01	133.21
s	6.98	114.80
t	–	164.40

heteronuclear cross correlation (HETCOR) experiment to determine which protons are on which carbons. The HETCOR was acquired as a 128 x 2K data set, used Gaussian apodization in both dimensions and it was zero filled to 256 in T_1. This experiment is analogous to the ^1H COSY, but since the axes are not the same there are no 'diagonal' correlations. Rather, contours appear where the ^1H and ^{13}C resonances are J-coupled to one another, i.e. a specific C-H pair. To summarize, by combining the ^1H and ^{13}C chemical shift information, the COSY homonuclear ^1H information on neighbouring groups and the HETCOR information which tells us which protonated carbons are neighbours we were able to assign the entire spectrum. The results are consistent with the proposed PSHQ10 structure.

We have determined the weight-average molecular weight (M_w) of PSHQ10 using g.p.c. In the present study we employed two different PSHQ10s, one having M_w of 45000 relative to polystyrene standards and a polydispersity index of 2, and the other having a M_w of 35000 relative to polystyrene standards and a polydispersity index of 2. Unless stated explicitly, the results presented below are based on the PSHQ10 specimens with $M_w = 45000$.

Sample preparation

Specimens for rheological measurements were prepared by first dissolving PSHQ10 in dichloromethane as solvent in the presence of an antioxidant (Irganox 1010, Ciba-Geigy Group) and then slowly evaporating the solvent at room temperature for 1 week. The cast films (1 mm thick) were further dried in a vacuum oven at room temperature for at least 3 weeks and at 90°C for 48 h. Immediately before the rheological measurement, the specimen with $M_w = 45000$ was further dried at 120°C for 2 h to remove any residual solvent and moisture.

Rheological measurement

A model R16 Weissenberg rheogoniometer (Sangamo Control, Inc.) in the cone-and-plate (25 mm diameter plate and 4° cone angle) configuration was used to measure, (1) in the steady-state shear mode, the shear stress (σ) as a function of shear rate ($\dot{\gamma}$), and (2) in the oscillatory shear mode, the dynamic storage modulus (G') and dynamic loss modulus (G'') as a function of angular frequency (ω), under isothermal conditions. From the measurements of G' and G'', the absolute value of complex viscosity was calculated using the relationship:

$$|\eta^*(\omega)| = \{[G'(\omega)/\omega]^2 + [G''(\omega)/\omega]^2\}^{1/2}$$

Strain amplitude was varied from 0.01 to 0.06, which was well within the linear viscoelastic range of the materials investigated. This, together with data acquisition during measurement, was accomplished with the aid of a microcomputer interfaced with the rheometer. All experiments were conducted in the presence of nitrogen in order to preclude oxidative degradation of the specimen. Temperature control was satisfactory to within ±1°C.

Thermal transitions of PSHQ10

Thermal transition temperatures of the synthesized PSHQ10 were determined by d.s.c. (Perkin-Elmer DSC-7). *Figure 1* shows a d.s.c. trace during the first heating cycle for a solvent-cast PSHQ10 specimen with $M_w = 45000$, which was annealed at 160°C for 20 h. D.s.c. runs were made under a nitrogen atmosphere with heating and cooling rates of 20°C min^{-1}. It can be seen from *Figure 1* that PSHQ10 has (1) a glass transition transition of ~88°C, (2) a melting point of ~115°C, and (3) a T_{NI} of ~175°C. Before embarking on the present study, we spent a considerable amount of effort[22] in trying to understand the effect of thermal history on the rheological behaviour of PSHQ10.

RESULTS AND DISCUSSION

Oscillatory shear flow properties of PSHQ10 in the isotropic region

The oscillatory shear flow properties of PSHQ10 in the isotropic region were measured at 180, 185 and 192°C, and are summarized in terms of reduced

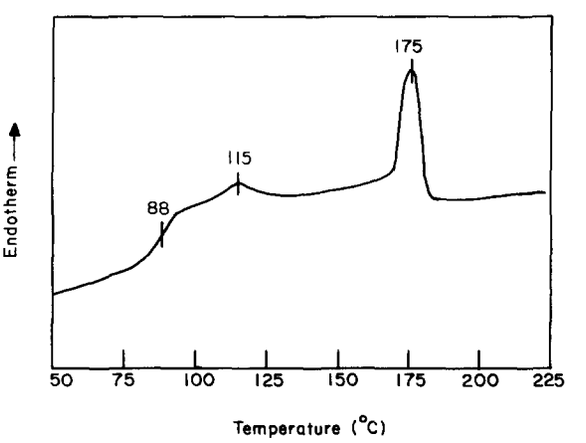

Figure 1 D.s.c. trace for a solvent-cast PSHQ10 specimen, which was annealed at 160°C for 20 h, showing that (1) the glass transition temperature is 88°C, (2) the melting temperature is 115°C, and (3) the nematic-to-isotropic transition temperature is 175°C

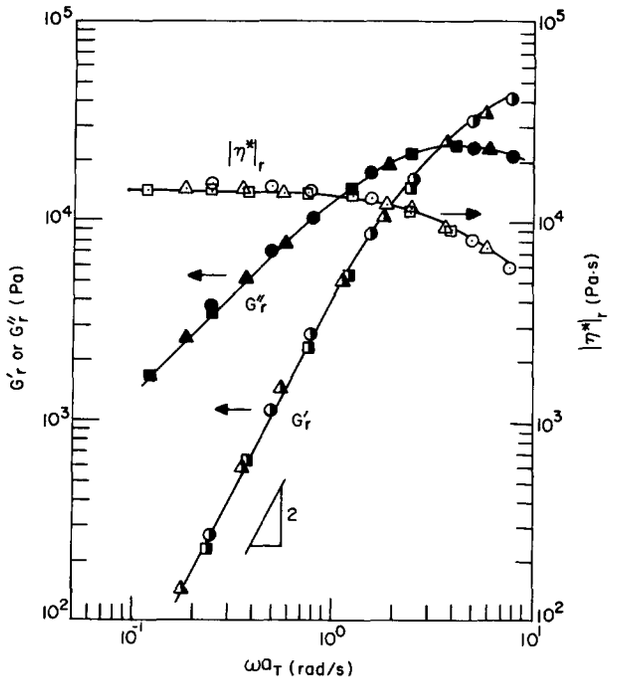

Figure 2 Reduced plots for $\log G'_r$ *versus* $\log \omega a_T$ at: (◐) 180°C, (▲) 185°C, (■) 192°C; $\log G''_r$ *versus* $\log \omega a_T$ at: (●) 180°C, (▲) 185°C, (■) 192°C; and $\log |\eta^*|$ *versus* $\log \omega a_T$ at: (⊙) 180°C, (△) 185°C, (⊡) 192°C for PSHQ10 in the isotropic region. The reference temperature used is 180°C

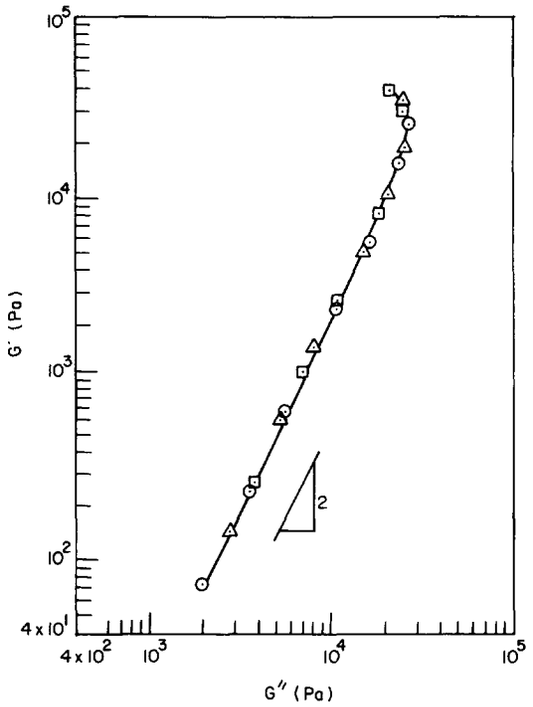

Figure 3 Plots of $\log G'$ *versus* $\log G''$ for PSHQ10 in the isotropic region at: (⊙) 192°C; (△) 185°C; (⊡) 180°C

variables in *Figure 2*: $G'_r = G'\rho_0 T_0/\rho T$, $G''_r = G''\rho_0 T_0/\rho T$, and $|\eta^*|_r = |\eta^*|\rho_0 T_0/\rho T$. Note in *Figure 2* that a_T is a shift factor and the subscript 0 denotes a reference state. A close look at *Figure 2* reveals that although PSHQ10 is a semiflexible polymer, the essential features of the reduced plots are little different from those often observed for flexible macromolecules[23].

Plots of $\log G'$ *versus* $\log G''$ for PSHQ10 in the isotropic region are given in *Figure 3*, showing a temperature-independent correlation. On the basis of the previous studies of Han and co-workers[24–29], we can conclude from *Figure 3* that the data were indeed taken in the isotropic region. This then assures us that the time–temperature superposition used in *Figure 2* is justified. When discussing the oscillatory shear flow properties of PSHQ10 in the nematic region below, we shall make use of the rheological significance of *Figure 3*.

Oscillatory shear flow properties of PSHQ10 in the nematic region

Effect of thermal history. For this experiment, PSHQ10 with $M_w = 35\,000$ was employed. In order to investigate how annealing conditions might influence the oscillatory shear flow properties of PSHQ10 in the nematic region, we varied the time of annealing after a specimen was placed in the cone-and-plate fixture at a temperature below the T_{NI} of PSHQ10. Plots of $\log G'$ *versus* $\log \omega$ are given in *Figure 4*, and plots of $\log G''$ *versus* $\log \omega$ are given in *Figure 5*, at 140°C for PSHQ10 specimens having the following thermal histories: (1) a solvent-cast specimen which was annealed at 140°C for 2 h; (2) a solvent-cast specimen which was annealed at 140°C for 4.5 h; (3) a solvent-cast specimen which was annealed at 140°C for 24 h; and (4) a solvent-cast specimen which was first annealed at 140°C for 24 h and then thermally treated at 200°C for 30 min, and finally cooled very slowly down to 140°C for further annealing for a period of 24 h. Note that a fresh specimen was used for each frequency sweep.

The seemingly complicated frequency dependencies of G' and G'' for PSHQ10 in the nematic region at 140°C, displayed in *Figures 4* and *5*, can easily be explained by using the well-established frequency dependencies of G' and G'' for viscoelastic fluids over a wide range of ω

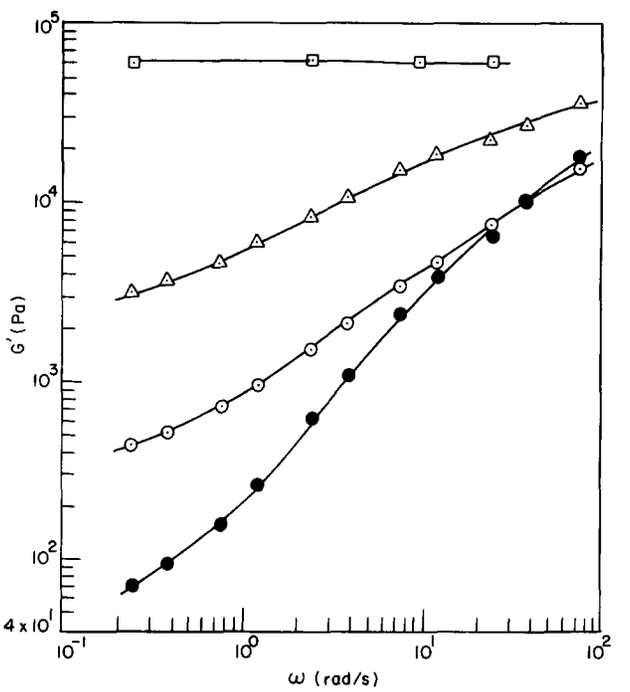

Figure 4 Plots of $\log G'$ *versus* $\log \omega$ at 140°C for solvent-cast PSHQ10 specimens having the following thermal histories: (⊙) annealed at 140°C for 2 h; (△) annealed at 140°C for 4.5 h; (⊡) annealed at 140°C for 24 h; (●) first annealed at 140°C for 24 h and then heated to 200°C, held there for 30 min, subsequently cooled slowly down to 140°C and annealed there for 24 h

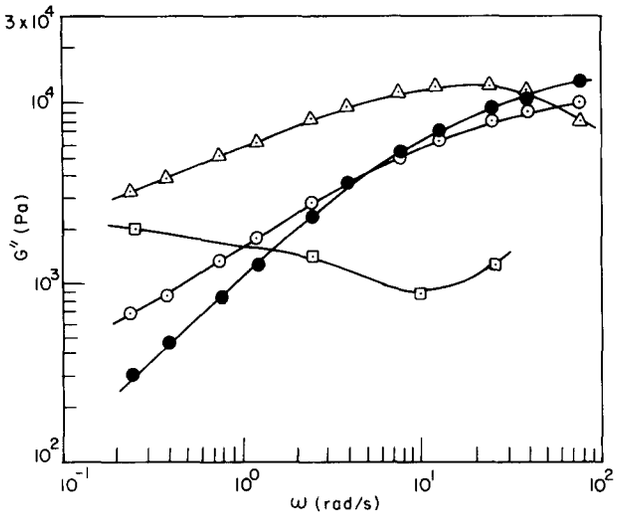

Figure 5 Plots of $\log G''$ *versus* $\log \omega$ at 140°C for solvent-cast PSHQ10 specimens having the same thermal histories as the specimens in *Figure 4*

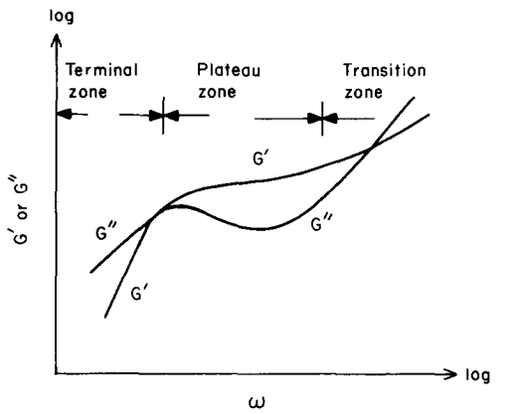

Figure 6 Schematic diagram of plots of $\log G'$ *versus* $\log \omega$ and $\log G''$ *versus* $\log \omega$ for viscoelastic polymeric liquids over a wide range of angular frequencies

(*Figure 6*)[23]. Specifically, the following observations are worth noting; (1) $\log G'$ *versus* $\log \omega$ and $\log G''$ *versus* $\log \omega$ plots for the specimens which were annealed at 140°C for 2 and 4.5 h, respectively, lie in the terminal region; (2) $\log G'$ *versus* $\log \omega$ and $\log G''$ *versus* $\log \omega$ plots for the specimen which received thermal treatment at 200°C and subsequently annealed at 140°C, also lie in the terminal region; (3) $\log G'$ *versus* $\log \omega$ and $\log G''$ *versus* $\log \omega$ plots for the specimen which was annealed at 140°C for 24 h, lie in the plateau region. The above observations indicate that as annealing continues, the structure of PSHQ10 in the nematic region changes with time, giving rise to different viscoelastic responses.

Using the data given in *Figures 4* and *5*, we prepared the plots of $\log G'$ *versus* $\log G''$ and they are given in *Figure 7*. It can be seen from *Figure 7* that the thermal history of a specimen greatly influences not only the shape of $\log G'$ *versus* $\log G''$ plots, but also the magnitude of G' for a fixed value of G'', namely the value of G' increases with increasing annealing time. Recall that $\log G'$ *versus* $\log G''$ plots of PSHQ10 in the isotropic region are independent of temperature (see *Figure 3*). This then suggests that $\log G'$ *versus* $\log G''$ plots are very sensitive to the thermal history, which in turns affects the morphology of PSHQ10 specimens in the nematic region. In other words, $\log G'$ *versus* $\log G''$ plots are sensitive to variations in the morphological state of PSHQ10 (and also of TLCPs in general). We can also conclude from *Figure 7* that the melt elasticity (i.e. values of G' for a fixed value of G'') of a specimen which received thermal treatment in the isotropic region at 200°C is less than that of the specimens which did not receive thermal treatment in the isotropic region.

It is appropriate to mention at this juncture that earlier Han and Kim[30] analysed the rheological data of Aoki[31] who reported the oscillatory shear flow properties of poly(acrylonitrile-*stat*-butadiene-*stat*-styrene) (ABS) resins containing various amounts of rubber particles, and showed that $\log G'$ *versus* $\log G''$ plots were very sensitive to the amounts of rubber particles present in the ABS resins, i.e. the greater the amount of rubber particles in an ABS resin, the larger the values of G' (i.e. the more elastic). Also, when investigating the rheological behaviour of microphase-separated block copolymers, and mixtures of a microphase-separated block copolymer and a homopolymer, Han and co-workers[30,32–35] observed the temperature dependence of $\log G'$ *versus* $\log G''$ plots, very similar to that given in *Figure 7*. On the basis of these observations, we can conclude from *Figure 7* that the solvent-cast PSHQ10 specimens, which were subjected to different thermal histories, must have had different morphological states.

Plots of $\log |\eta^*|$ *versus* $\log \omega$ are given in *Figure 8*. The following observations are worth noting: (1) the specimen, which was annealed at 140°C for 2 h, exhibits shear-thinning behaviour over the entire range of ω tested; (2) shear-thinning behaviour becomes more intense as the annealing period increased from 2 to 4.5 h and to 24 h; (3) when a solvent-cast specimen received thermal treatment at 200°C for 30 min and subsequently was annealed at 140°C for 24 h, plots of $\log |\eta^*|$ *versus* $\log \omega$ exhibit (i) a very weak shear-thinning region at low ω, (ii) a Newtonian plateau region at intermediate values of ω, and (iii) a strong shear-thinning region at high ω. Of

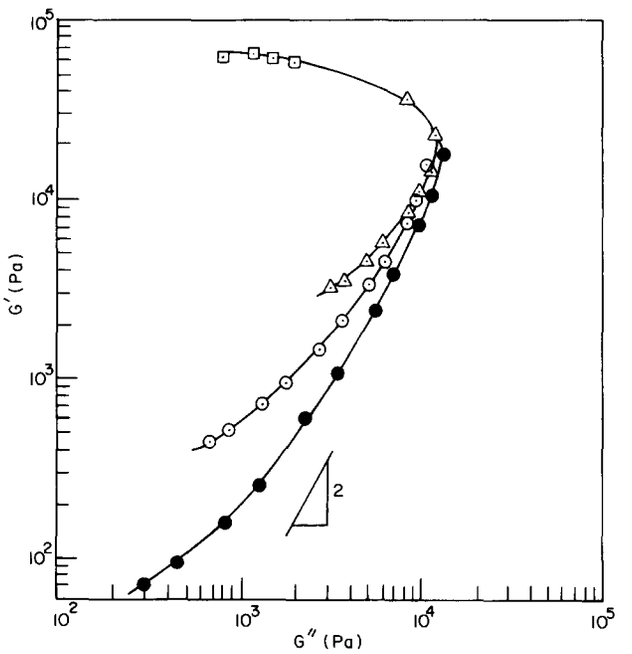

Figure 7 Plots of $\log G'$ *versus* $\log G''$ at 140°C for solvent-cast PSHQ10 specimens, having the same thermal histories as the specimens in *Figure 4*

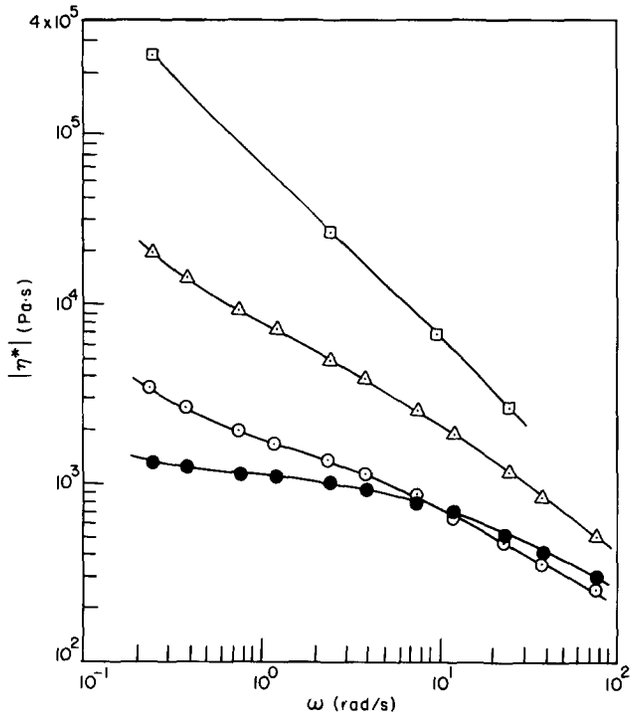

Figure 8 Plots of $\log|\eta^*|$ *versus* $\log\omega$ at 140°C for solvent-cast PSHQ10 specimens having the same thermal histories as the specimens in *Figure 4*

particular note in *Figure 8* is that at low ω the specimen which received thermal treatment at a temperature above T_{NI} has much lower values of $|\eta^*|$ than the one which did not receive such a thermal treatment in the isotropic region. In other words, the thermally treated specimen appears to exhibit a three-region viscosity curve, observed earlier by Onogi and Asada[36].

We believe that the complicated frequency dependence of $|\eta^*|$, observed in *Figure 8*, is attributable to the differences in the morphology that existed in specimens, which had experienced different thermal histories. Similar observations were reported earlier by Lin and Winter[37], who used a thermotropic copolyester of HBA and HNA. It should be mentioned, however, that owing to the fact that the T_{NI} of the HBA/HNA copolyester was above or close to its thermal degradation temperature (~400°C), in the study of Lin and Winter[37] it was not possible to heat samples to an isotropic state before being subjected to oscillatory shear flow measurements in an anisotropic state. In a previous study[22], using d.s.c. we observed the formation of a 'crystal-like' phase when PSHQ10 was annealed at temperatures in the nematic region between 130°C and 140°C and the disappearance of the 'crystal-like' phase when PSHQ10 was first heated to an isotropic state and then subsequently cooled down to an anisotropic state. This then explains why in *Figure 8* the $|\eta^*|$ of the specimen which was annealed at 140°C without receiving thermal treatment at an isotropic state at 200°C, increased with increasing annealing time. On the other hand, the values of $|\eta^*|$ for the specimen which received thermal treatment at 200°C are lower than those of the specimens that did not receive thermal treatment at an isotropic state. This seems to suggest that the morphology of the specimen which received thermal treatment at an isotropic state is quite different from that of the specimens which did not receive such thermal treatment. The details of the effect of thermal history on the rheological behaviour of PSHQ10 are referred to in our previous paper[22].

Hysteresis. For this experiment, PSHQ10 with $M_w = 35000$ was employed. The measurements of $|\eta^*|$ by increasing or decreasing ω for a solvent-cast specimen, which was annealed for 443 h at 150°C, are given in *Figure 9*, where open circles represent the data taken by increasing ω stepwise (ascending frequency sweep) and filled circles represent the data taken by decreasing ω stepwise (descending frequency sweep). It can be seen in *Figure 9* that the values of $|\eta^*|$ for the descending frequency sweep are lower than those for the ascending frequency sweep, indicating that the PSHQ10 specimen exhibits a hysteresis effect in the measurement of oscillatory shear flow properties. Earlier, similar observations were made by Wissbrun[2], who used thermotropic copolyesters.

Figure 10 describes the measurements of $|\eta^*|$ as functions of ω for specimens having the following thermal

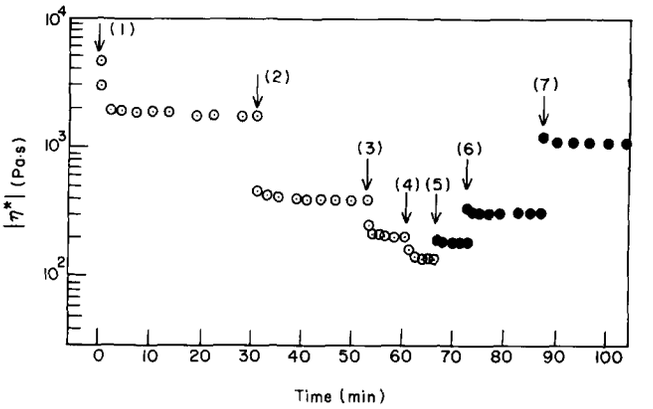

Figure 9 Hysteresis effect observed in the complex viscosity of a solvent-cast PSHQ10 specimen, which was annealed at 150°C for 443 h: (○) data taken for ascending frequency sweep; (●) data taken for descending angular frequency sweep. The arrows indicate the time at which the angular frequency was increased for ascending frequency sweep or decreased for descending frequency sweep. ω (rad s^{-1}): (1) 0.24; (2) 2.37; (3) 9.45; (4) 23.7; (5) 9.45; (6) 2.37; (7) 0.24

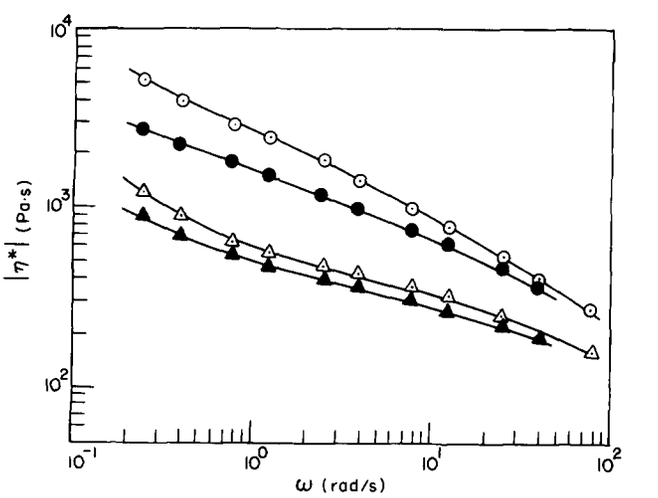

Figure 10 Plots of $\log|\eta^*|$ *versus* $\log\omega$ for solvent-cast PSHQ10 specimens having the following thermal histories: (⊙, ●) first annealed at 140°C for 3 h and then heated to 150°C for further annealing for 80 h; (△, ▲) thermally treated at 190°C for 30 min and then cooled slowly down to 150°C. Open symbols represent the data taken for the ascending frequency sweep, and filled symbols represent the data taken for the descending frequency sweep

histories: (1) a solvent-cast specimen was first annealed at 140°C for 3 h and then at 150°C for 80 h, and (2) a solvent-cast specimen was first heated into the isotropic region at 190°C for 30 min and then cooled very slowly down to the nematic region at 150°C. It can be seen from *Figure 10* that, as compared to the specimen which was annealed into the nematic region at 140°C, the specimen which first received thermal treatment in the isotropic region at 190°C has: (i) lower values of $|\eta^*|$, (ii) less hysteresis effect, and (iii) less intense shear-thinning behaviour. From the above observations we conclude that the thermal history of a PSHQ10 specimen has a profound influence on the extent of the hysteresis effect in its rheological behaviour.

Control of initial morphology. In order to control the initial morphology of PSHQ10 in the nematic region, in the present study the following experimental procedures were adopted. (1) First, a solvent-cast PSHQ10 specimen was placed in the cone-and-plate fixture at 190°C, and after the temperature was equilibrated a steady shear flow at a rate of 0.085 s^{-1} was applied for 5 min to the specimen. Oscillatory shear flow measurements were then taken over a wide range of ω at 190°C. (2) The specimen was then cooled very slowly down to a predetermined temperature (130, 140, 150, 160 or 170°C) in the nematic region. It took ~1.5 h to cool the specimen from 190 to 140°C (there was no convective cooling device installed in the instrument). (3) After the temperature was equilibrated in the nematic region, the specimen was subjected to oscillatory shear flow over a wide range of ω. *Figure 11* gives plots of log G' *versus* log ω, and *Figure 12* gives plots of log G'' *versus* log ω, for PSHQ10 specimens at 130, 140, 150 and 160°C, respectively, after each of the specimens was cooled from the isotropic region. Note that a fresh specimen was used for each temperature. It can be seen in *Figure 11* that the shape of the log G' *versus* log ω plot very much resembles that for microphase-separated block copolymers[30,32,33], in that curvature is seen in the terminal region. This appears to suggest that at temperatures ranging from 130 to 160°C PSHQ10 is no longer a homogeneous polymer, which is

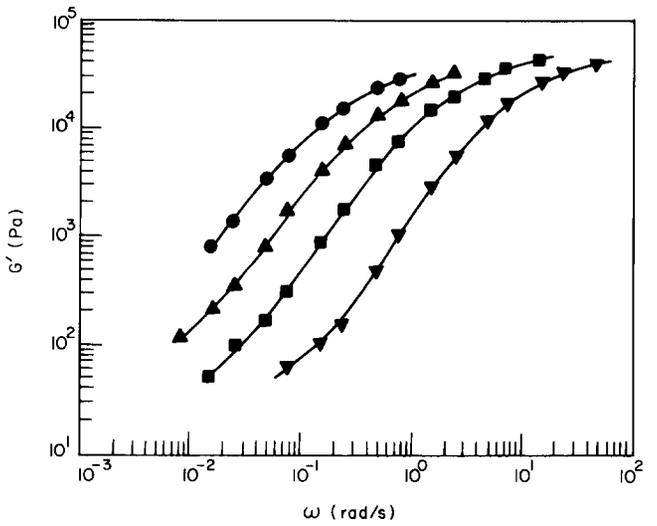

Figure 11 Plots of log G' *versus* log ω for solvent-cast PSHQ10 specimens after being thermally treated in the isotropic region at 190°C and then cooled slowly down to the nematic region at: (●) 130°C; (▲) 140°C; (■) 150°C; (▼) 160°C

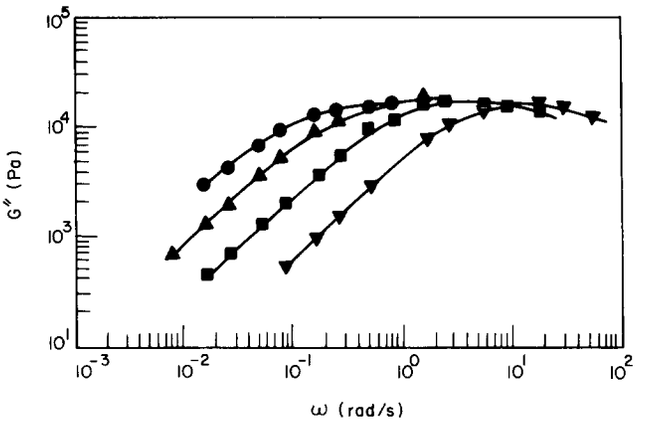

Figure 12 Plots of log G'' *versus* log ω for solvent-cast PSHQ10 specimens, which have the same thermal histories as the specimens in *Figure 11*

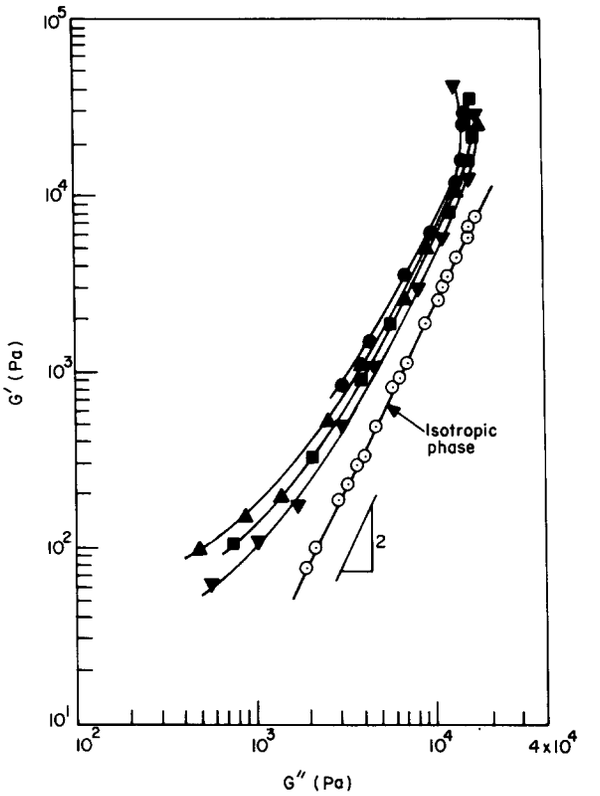

Figure 13 Plots of log G' *versus* log G'' for solvent-cast PSHQ10 specimens, which have the same thermal histories as the specimens in *Figure 11*, except for (⊙) which represents the data taken in the isotropic region at 190°C

expected to have a slope of 2 in the terminal region[23]. On the other hand, the shape of the log G'' *versus* log ω plot given in *Figure 12* does not show any unusual features which would be regarded as being distinctly different from those for homogeneous polymers. It should be mentioned that the specimens ($M_w = 35\,000$) used in *Figures 11* and *12* had thermal histories different from those used in *Figures 4*, *5*, *7* and *8*.

Using the data given in *Figures 11* and *12*, we have constructed the plots of log G' *versus* log G'' displayed in *Figure 13*, where for comparison plots of log G' *versus* log G'' for PSHQ10 in the isotropic region are also given. It is of interest to observe in *Figure 13* that log G' *versus* log G'' plots show temperature dependence, indicating that the morphology of PSHQ10 varies with temperature.

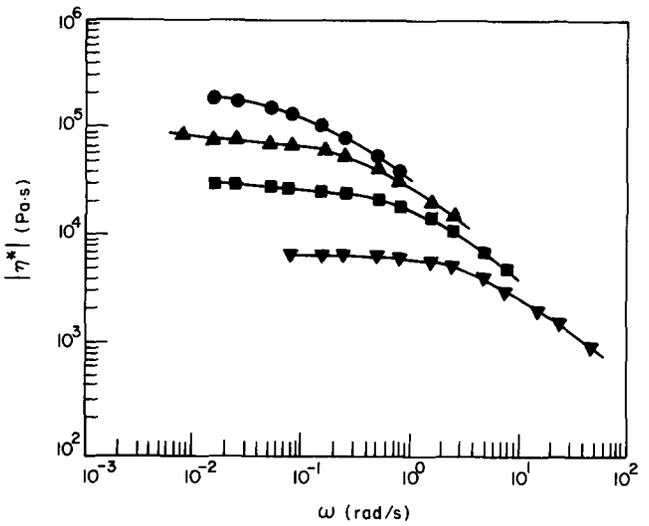

Figure 14 Plots of $\log|\eta^*|$ *versus* $\log\omega$ for solvent-cast specimens, which have the same thermal histories as the specimens in *Figure 11*

Note in *Figure 13* that as the temperature is increased from 130 to 160°C, $\log G'$ *versus* $\log G''$ plots move towards those in the isotropic region. Such temperature dependence of $\log G'$ *versus* $\log G''$ plots has been observed for microphase-separated block copolymers by Han and co-workers[30,32–35]. It can then be concluded that $\log G'$ *versus* $\log G''$ plots would be useful to determine the T_{NI} of TLCPs. What is significant about *Figure 13* is that $\log G'$ *versus* $\log G''$ plots are very sensitive to any variation in the structure of the polymer and thus can be used to monitor the initial morphology of the PSHQ10. In a separate study[38], we indeed used $\log G'$ *versus* $\log G''$ plots to monitor the initial morphology of PSHQ10 when conducting transient shear flow experiments.

Figure 14 gives plots of $\log|\eta^*|$ *versus* $\log\omega$ at 130, 140, 150 and 160°C for PSHQ10 specimens ($M_w = 35\,000$) after being cooled down from the isotropic region. Note that a fresh specimen was used for each temperature. We observe in *Figure 14* that at 130°C PSHQ10 exhibits shear-thinning behaviour over the entire range of ω tested, but the extent of shear-thinning behaviour becomes less as the temperature increases, and at 160°C a Newtonian plateau region appears at low ω and a shear-thinning region at higher ω. Note that *Figure 14* was prepared using the data given in *Figures 11* and *12*. The shape of the curve in *Figure 14*, especially at low values of ω, is affected much more by the magnitude of G'' than by the magnitude of G' because, according to *Figures 11* and *12*, at low values of ω the magnitude of G'' is much greater than that of G'. In view of the fact that the shape of the $\log G''$ *versus* $\log\omega$ plot, for instance, at 160°C given in *Figure 12* is very similar to that for homopolymers with flexible chains, it is not surprising to observe in *Figure 14* that the $\log|\eta^*|$ *versus* $\log\omega$ plot at 160°C very much resembles that for homopolymers with flexible chains. On the other hand, from the micrographs taken in our previous study[22] we know that PSHQ10 at 160°C has a liquid-crystalline phase in the form of a polydomain structure. We can thus conclude that the use of the $\log G'$ *versus* $\log G''$ plot is much more effective than the use of the $\log|\eta^*|$ *versus* $\log\omega$ plot, in determining whether a LCP is in the isotropic region or in the anisotropic region.

Temperature dependence of $|\eta^*|$. *Figure 15* gives plots of $\log|\eta^*|$ *versus* temperature for a PSHQ10 specimen at $\omega = 0.24$ rad s^{-1}. Note that the data points in *Figure 15* were obtained for specimens before being subjected to steady shear flow in the nematic region, and a sufficiently long time was allowed to attain temperature equilibrium. It can be seen in *Figure 15* that $|\eta^*|$ goes through a maximum at ~175°C, which is very close to the T_{NI} determined by d.s.c. under quiescent conditions, and that $|\eta^*|$ at 170°C is higher than that at 160°C. In reference to *Figure 15*, the temperature dependence of $|\eta^*|$ can be divided into three regions: (1) the nematic region, where $T < 165$°C and $|\eta^*|$ decreases with increasing temperature; (2) the biphasic region, where $165°C < T < 175°C$ and $|\eta^*|$ increases with increasing temperature; and (3) the isotropic region, where $T > 175$°C and $|\eta^*|$ decreases with increasing temperature. While the temperature dependence of $|\eta^*|$ in the isotropic region can be explained by the Arrhenius rule, the interpretation of the temperature dependence of $|\eta^*|$ in the nematic region is not as simple, due to the fact that the morphology of PSHQ10 varies with temperature. The increase of $|\eta^*|$ in the biphasic region is attributable as being due to the polydisperse nature of PSHQ10 (having a polydispersity index of ~2), since the low molecular weight portion of the specimen would begin to transform to the isotropic phase before reaching the T_{NI}, 175°C. Note that the viscosity of a TLCP is greater in the isotropic region than in the anisotropic region, because the anisotropic phase undergoes orientation in the shear direction. Therefore as the temperature is increased from ~165 to 175°C, the amount of isotropic phase in the bisphasic region will increase accordingly, thus increasing the weight-averaged viscosity of the mixture. It should be mentioned that the biphasic nature, as investigated by the rheological method, of other TLCPs was reported by other investigators[7,11].

Effect of steady shear flow. Let us now discuss how the application of steady shear flow might affect subsequent oscillatory shear flow properties of PSHQ10 in the nematic region. It should be remembered that in the present study the specimen, which was subjected

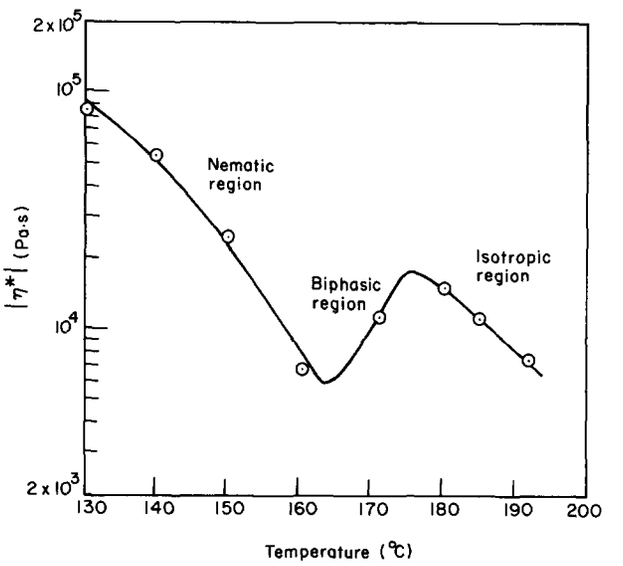

Figure 15 Temperature dependence of $|\eta^*|$ for PSHQ10 at $\omega = 0.24$ rad s^{-1}

to steady shear flow followed by oscillatory shear flow in the nematic region, had already received thermal treatment in the isotropic region and had been cooled to the nematic region. In the present study we measured the oscillatory shear flow properties of PSHQ10 specimens after they had been allowed to rest for a fixed period upon cessation of steady shear flow. During the rest period, reorganization or reformation of domain textures (often referred to as 'structural recovery') would take place in the specimens. It should be mentioned that in the past, small amplitude oscillatory deformations were used to monitor the time evolution of structural recovery, in terms of complex viscosity $|\eta^*|$ under small amplitude oscillatory deformations, in lyotropic or thermotropic LCPs after cessation of transient or steady shear flow[14,39]. Such experiments were conducted on the premise that the morphology of the specimen would not be altered by the small amplitude oscillatory deformations applied to the specimen. Very recently we also conducted similar experiments using PSHQ10 and the details of the study will be reported in a future publication.

Figure 16 describes the effect of steady shear flow on subsequent oscillatory shear flow property, $|\eta^*|$, for PSHQ10 specimens at 150°C, where a fresh specimen was used for each shear rate. Also given in *Figure 16*, for comparison, are plots of $\log|\eta^*|$ *versus* $\log\omega$ for an *unsheared* PSHQ10 specimen (i.e. before being subjected to steady shear flow). It can be seen in *Figure 16* that the application of steady shear flow decreased the $|\eta^*|$ of a specimen, and that as the applied shear rate increased, the values of $|\eta^*|$ *after* shearing approached those *before* shearing.

Figure 17 shows $\log G'$ *versus* $\log G''$ plots at 150°C for PSHQ10 specimens after being sheared at a shear rate of 0.107, 0.526 and 1.07 s^{-1}. Note that a fresh specimen was used for each shear rate. Also plotted in *Figure 17*, for comparison, are $\log G'$ *versus* $\log G''$ plots at 150°C for a PSHQ10 specimen before being sheared and for a PSHQ10 specimen in the isotropic region at 190°C. It can be seen that the application of steady shear flow

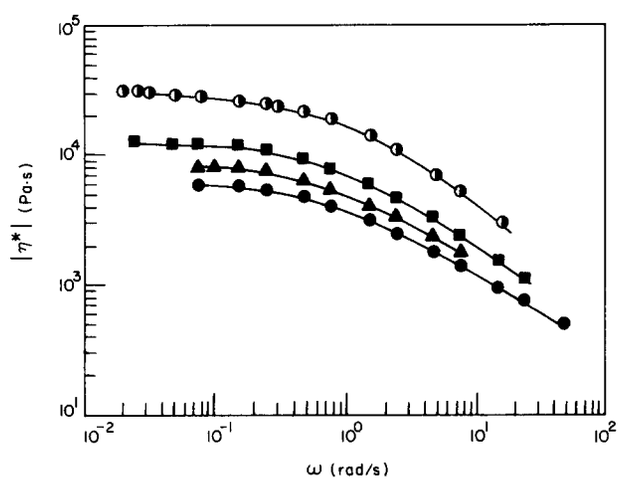

Figure 16 Effect of steady shear flow on subsequent complex viscosity of PSHQ10 specimens at 150°C. Oscillatory shear measurements were taken after a specimen was subjected to steady shear flow at shear rates (s^{-1}): (●) 0.107; (▲) 0.536; (■) 1.07. A fresh specimen was used for each shear rate. Upon cessation of steady shear flow, the specimen was allowed to rest for 3 h before oscillatory shear measurement began. (◑) Data taken using *unsheared* specimens (i.e. before being subjected to steady shear flow)

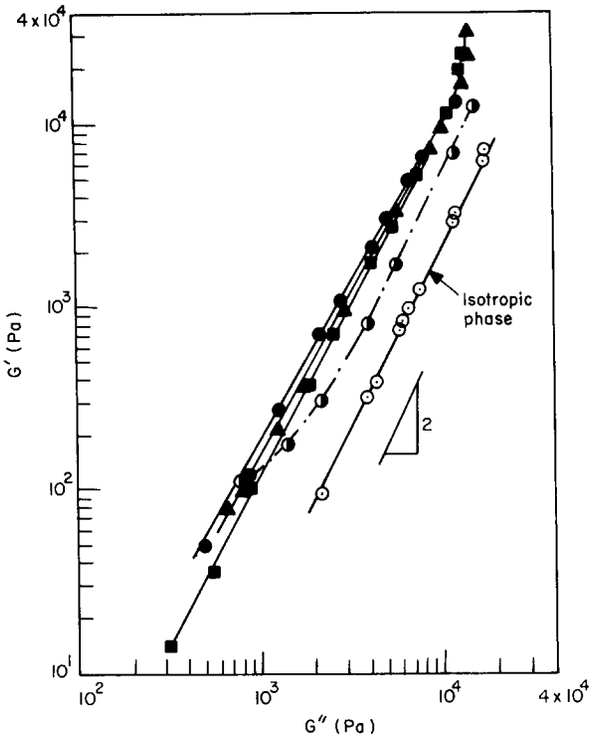

Figure 17 Effect of steady shear flow on subsequent oscillatory shear flow properties, shown by $\log G'$ *versus* $\log G''$ plots, for PSHQ10 specimens at 150°C. The shear histories are the same as the specimens in *Figure 16*. Symbols have the same meanings as in *Figure 16*, except for (⊙) which represents the data taken in the isotropic region at 190°C

shifted the $\log G'$ *versus* $\log G''$ plot in the nematic region farther away from that in the isotropic region, implying that the structure of the *sheared* specimen was driven to a stronger anisotropic state. It is of interest to observe in *Figure 17* that as the applied shear rate is increased from 0.107 to 1.07 s^{-1}, the $\log G'$ *versus* $\log G''$ plot of the *sheared* specimen moves towards that of the *unsheared* specimen. We can thus conclude that $\log G'$ *versus* $\log G''$ plots are very sensitive to variations, as affected by the extent of steady shear flow, in the morphology of PSHQ10.

Notice in *Figure 17* that the $\log G'$ *versus* $\log G''$ plot in the *terminal* region of PSHQ10 specimens before being sheared has curvature, closely resembling that observed in the liquid–liquid, two-phase mixtures consisting of a block copolymer and a homopolymer[34,35]. However, the $\log G'$ *versus* $\log G''$ plot of a *sheared* specimen no longer has curvature, resembling that often observed in homogeneous polymers[24–29]. This is further evidence that the application of shear flow to PSHQ10 has altered its morphology, producing a more uniform morphology which is close to a monodomain texture, as compared to polydomain textures that existed prior to shearing.

Cox–Merz rule for PSHQ10. It has been reported extensively, since the first study of Cox and Merz[40], that $\log|\eta^*|$ *versus* $\log\omega$ plots can be correlated with the logarithmic plots of steady shear viscosity (η) *versus* shear rate ($\dot{\gamma}$). Such a correlation has been obtained primarily for homogeneous polymer systems. In the present study, we investigated whether the Cox–Merz rule holds for PSHQ10 in both the isotropic and nematic regions. *Figure 18* gives plots of $\log|\eta^*|$ *versus* $\log\omega$ and $\log\eta$ *versus* $\log\dot{\gamma}$ for PSHQ10 at 190°C, showing that the Cox–Merz rule holds for PSHQ10 in the *isotropic* region.

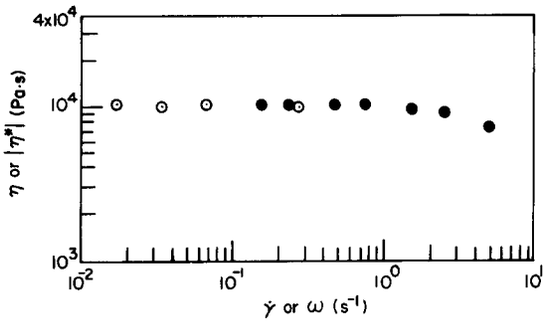

Figure 18 Plots of $\log|\eta^*|$ *versus* $\log\omega$ (●), and plots of η *versus* $\log\dot{\gamma}$ (⊙) for PSHQ10 specimens in the isotropic region at 190°C

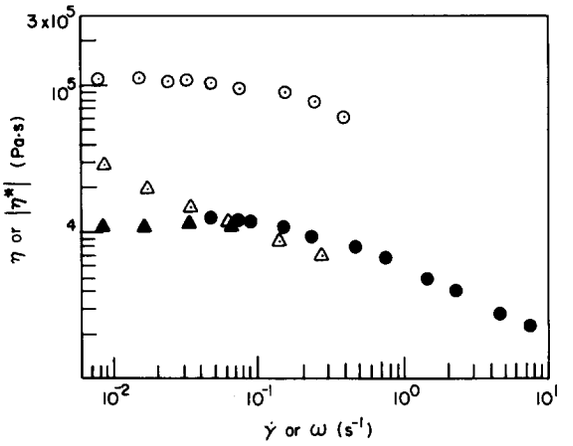

Figure 19 Plots of $\log|\eta^*|$ *versus* $\log\omega$ at 140°C for a thermally treated PSHQ10 specimen: (⊙) before being subjected to steady shear flow; (●) after being subjected to steady shear flow. Plots of $\log\eta$ *versus* $\log\dot{\gamma}$ at 140°C for a thermally treated PSQH10 specimen: (△) during the first shear rate sweep; (▲) during the second shear rate sweep

Plots of $\log|\eta^*|$ *versus* $\log\omega$ and $\log\eta$ *versus* $\log\dot{\gamma}$ are given in *Figure 19* for a PSHQ10 specimen in the nematic region at 140°C. The thermal history and experimental procedures utilized to obtain the results in *Figure 19* are as follows: (1) a specimen, which had received thermal treatment at 190°C, was cooled down slowly to 140°C, and then after a rest for 2 h the specimen was subjected to a frequency sweep; (2) after completion of the frequency sweep, the specimen was subjected to steady shear flow by increasing $\dot{\gamma}$ from 0.0085 to 0.269 s^{-1}; (3) after a rest for 1 h upon cessation of the previous shear flow, the specimen was subjected to steady shear flow once again by increasing $\dot{\gamma}$ from 0.0085 to 0.034 s^{-1}; (4) after completion of the steady shear flow the specimen was subjected to a frequency sweep once again; and (5) finally, the specimen was subjected to steady shear flow again at $\dot{\gamma} = 0.068\ s^{-1}$.

The following observations are worth noting in *Figure 19*. The shape of the $\log|\eta^*|$ *versus* $\log\omega$ curve *after* steady shear flow is almost the same as that *before* steady shear flow, but the values of $|\eta^*|$ *after* steady shear flow are about an order of magnitude smaller than those *before* steady shear flow. When the specimen was subjected to steady shear flow for the first time, η decreased rapidly with increasing $\dot{\gamma}$, exhibiting shear-thinning behaviour over the entire range of $\dot{\gamma}$ tested which is believed to be due to the presence of polydomains in the specimen. But when the specimen was subjected to steady shear flow for a second time, $\log\eta$ *versus* $\log\dot{\gamma}$ plots showed a Newtonian plateau region. Thus, by comparing the $|\eta^*|$ data obtained from the rest state with the η data obtained in the first shear rate sweep we conclude that the Cox–Merz rule does *not* hold. However, when comparing the $|\eta^*|$ data obtained after the specimen was subjected to steady shear flow with the η data obtained in the second shear rate sweep, we can conclude that the Cox–Merz rule seems to hold. In other words, the Cox–Merz rule does *not* hold for a PSHQ10 specimen having polydomains, while it seems to hold after polydomains have been broken up under steady shear flow. This observation is expected to hold for other TLCPs as well. Therefore, we can conclude that the morphological state of a TLCP specimen in the nematic region plays an important role in determining whether or not the Cox–Merz rule holds.

CONCLUSIONS

In the present study we investigated the oscillatory shear flow properties of an aromatic thermotropic polyester (PSHQ10) in both the isotropic and nematic regions, placing emphasis on the effects of thermal and shear histories. We found that when an as-cast PSHQ10 specimen was annealed at a temperature below its T_{NI}, the rheological properties varied continuously during the experiment and thus it was not possible to obtain meaningful rheological measurements in the nematic region of the TLCPs. We have shown that it would not be possible to investigate the effect of shear history on the rheological properties of a TLCP in the nematic region *unless* the effect of thermal history is suppressed or isolated. This was made possible in the present study, since the initial morphology of a PSHQ10 specimen was controlled by first heating to the isotropic region and then cooling slowly down to a predetermined temperature in the nematic region. In other words, thermal treatment in the isotropic region followed by a very slow cooling to the nematic region enabled us to control the initial morphology of PSHQ10 specimen in the nematic region. It should be mentioned that earlier Driscoll and co-workers[15] reported the oscillatory shear flow properties of a thermotropic polyester, having a chemical structure very similar to PSHQ10, in both the isotropic and nematic regions. However, they did not report the effect of thermal history (i.e. annealing temperature and annealing period) on the rheological behaviour of the polymer in the nematic region.

In this study we observed that in the nematic region the PSHQ10 specimen, which had not received thermal treatment in the isotropic state, exhibited a hysteresis effect during oscillatory shear flow, namely the values of $|\eta^*|$ for ascending frequency sweep were not the same as those for descending frequency sweep. We found that the application of steady shear flow to a PSHQ10 specimen in the nematic region has a profound influence on subsequent oscillatory shear flow properties. Thus extreme care must be exercised when comparing oscillatory shear flow properties of TLCPs obtained by different research laboratories, *unless* the shear and thermal histories of the specimens were identical.

Finally, we found that the Cox–Merz rule holds for PSHQ10 in the isotropic region and the morphological state of a specimen in the nematic region determines whether or not the Cox–Merz rule holds. We observed that the morphology of PSHQ10 in the nematic region

is greatly influenced by the application of steady shear flow, which in turn influences subsequent oscillatory shear flow properties. We thus conclude that the Cox–Merz rule is not expected to hold when the morphological state of a TLCP is not the same during both steady shear flow and oscillatory shear flow.

REFERENCES

1 Jackson, W. J. and Kuhfuss, H. F. *J. Polym. Sci., Polym. Chem. Edn* 1976, **14**, 2043
2 Wissbrun, K. F. *Br. Polym. J.* 1980, **13**, 163
3 Prasadarao, M., Pearce, E. M. and Han, C. D. *J. Appl. Polym. Sci.* 1982, **27**, 1343
4 Simoff, D. A. and Porter, R. S. *Mol. Cryst. Liq. Cryst.* 1982, **110**, 1
5 Gotsis, A. D. and Baird, D. G. *J. Rheol.* 1985, **29**, 539
6 Viola, G. G. and Baird, D. G. *J. Rheol.* 1986, **30**, 601
7 Wunder, S. L., Ramachandran, S., Cochanour, C. R. and Weinberg, M. *Macromolecules* 1986, **19**, 1696
8 Wissbrun, K. F., Kiss, G. and Cogswell, F. N. *Chem. Eng. Commun.* 1987, **53**, 149
9 Zhou, Z., Wu, X. and Wang, M. *Polym. Eng. Sci.* 1988, **28**, 136
10 Irwin, R. S., Sweeny, W., Gardner, K. H., Cochanour, C. R. and Weinberg, M. *Macromolecules* 1989, **22**, 1065
11 Gonzalez, J. M., Minoz, M. E., Cortazar, M., Santamaria, A. and Pena, J. J. *J. Polym. Sci., Polym. Phys. Edn* 1990, **28**, 1533
12 Kalika, D. S., Giles, D. W. and Denn, M. M. *J. Rheol.* 1990, **34**, 139
13 Cocchini, F., Nobile, M. R. and Acierno, D. *J. Rheol.* 1991, **35**, 1171
14 Guskey, S. M. and Winter, H. H. *J. Rheol.* 1991, **35**, 1191
15 Driscoll, P., Masuda, T. and Fujiwara, K. *Macromolecules* 1991, **24**, 1567
16 Wissbrun, K. F. and Griffin, A. C. *J. Polym. Sci., Polym. Phys. Edn* 1982, **20**, 1835
17 Blumstein, A., Thomas, O. and Kumar, S. *J. Polym. Sci., Polym. Phys. Edn* 1986, **24**, 27
18 Sun, T., Lin, Y. G., Winter, H. H. and Porter, R. S. *Polymer* 1989, **3**, 1257
19 Furukawa, A. and Lenz, R. W. *Macromol. Chem. Macromol. Symp.* 1986, **2**, 3
20 Driscoll, P., Fujiwara, K., Masuda, T., Furukawa, A. and Lenz, R. W. *Polym. J.* 1988, **20**, 351
21 Driscoll, P., Masuda, T., Furukawa, A., Lenz, R. W. and Bhattacharya, S. *Polym. J.* 1990, **22**, 609
22 Kim, S. S. and Han, C. D. *Macromolecules* 1993, **26**, 3176
23 Ferry, J. D. 'Viscoelastic Properties of Polymers', 3rd Edn, Wiley, New York, 1980
24 Han, C. D. and Jhon, M. S. *J. Appl. Polym. Sci.* 1986, **32**, 3809
25 Han, C. D. and Lem, K. W. *Polym. Eng. Rev.* 1983, **2**, 135
26 Chuang, H. K. and Han, C. D. *J. Appl. Polym. Sci.* 1984, **29**, 2205
27 Han, C. D. and Chuang, H. K. *J. Appl. Polym. Sci.* 1985, **30**, 443
28 Han, C. D. and Yang, H. H. *J. Appl. Polym. Sci.* 1987, **33**, 1199
29 Han, C. D. *J. Appl. Polym. Sci.* 1988, **35**, 167
30 Han, C. D. and Kim, J. *J. Polym. Sci., Polym. Phys. Edn* 1987, **25**, 1741
31 Aoki, Y. *Rheol. J. (Japan)* 1979, **7**, 20
32 Han, C. D., Kim, J. and Kim, J. K. *Macromolecules* 1989, **22**, 383
33 Han, C. D., Baek, D. M. and Kim, J. K. *Macromolecules* 1990, **23**, 561
34 Kim, J., Han, C. D. and Chu, S. G. *J. Polym. Sci., Polym. Phys. Edn* 1988, **26**, 677
35 Han, C. D., Kim, J., Baek, D. M. and Chu, S. G. *J. Polym. Sci., Polym. Phys. Edn* 1990, **28**, 315
36 Onogi, S. and Asada, T. in 'Rheology' (Eds G. Astarita, G. Marrucci and L. Nicolais), Vol. 1, Plenum Press, New York, 1980, p. 127
37 Lin, Y. G. and Winter, H. H. *Macromolecules* 1988, **21**, 2439; 1991, **24**, 2877
38 Kim, S. S. and Han, C. D. *J. Rheol.* 1993, **37**, 847
39 Grizzuti, N., Cavella, S. and Cicarelli, P. *J. Rheol.* 1990, **34**, 1293
40 Cox, W. P. and Merz, E. H. *J. Polym. Sci.* 1958, **28**, 619